



Long-term effects of mineral precipitation on process performance, granules' morphology and microbial community in anammox granular sludge

C. Polizzi^{a,*}, T. Lotti^a, A. Ricoveri^b, R. Campo^a, C. Vannini^b, M. Ramazzotti^c, D. Gabriel^d, G. Munz^a

^a Department of Civil and Environmental Engineering, University of Florence, Via di S. Marta, 3, 50139 Firenze, Italy

^b Department of Biology University of Pisa, Via A. Volta 4, 56126 Pisa, Italy

^c Department of Biomedical, Experimental and Clinical Sciences "Mario Serio" University of Florence, Viale Morgagni 50, 50134 Firenze, Italy

^d GENOCOV Research group, Department of Chemical, Biological and Environmental Engineering, Escola d'Enginyeria, Universitat Autònoma de Barcelona, 08193 Bellaterra, Spain

ARTICLE INFO

Editor: Yang Liu

Keywords:

Anammox
Granular sludge
Mineral precipitation
Long-term stability

ABSTRACT

When treating wastewaters prone to inert precipitation with granular sludge systems, mineral formation needs to be properly controlled to ensure system's long-term stability. In this work, an extensive study on mineral precipitation on the surface of anammox granular sludge is presented. A 7-L reactor was inoculated with one-year stored biomass and volumetric load up to 0.48 gN-NO₂⁻/l/d were achieved, with nitrite removal above 95% and total nitrogen removal rate of almost 1 gN/l/d. Severe mineral precipitation was observed on the granules' surface after three months of hard-water feeding and resulted in a dramatic deterioration of reactor performance and biomass activity. Substrate diffusion limitation in the inner layers, insufficient mixing due to higher granule density and biofilm erosion due to shear stress increase were deemed the main mechanisms that lead to progressive process disruption. Gravimetric selection was applied to discard granules affected by precipitation and allowed for process restoration. Microbial community analyses revealed that mineral composition possibly affected competition between "Ca. Brocadia" and "Ca. Kuenenia". The knowledge gathered in the present study details the dramatic consequences on process performance lead by severe mineral precipitation and it is presented as a warning for full-scale applications treating wastewaters prone to precipitation.

1. Introduction

Anaerobic ammonium oxidation (anammox, AMX) remains at the forefront of the innovative biological treatments for nitrogen removal, due to the significant contribution towards energy autarchy and resource optimization in wastewater treatment facilities. Its application to side-streams and to some industrial wastewater is considered an established technology and current implementations rely on the synergy of partial nitrification and anammox (PN/A) processes, allowing for a complete autotrophic nitrogen removal and a significant reduction in oxygen requirement compared to conventional treatments (nitrification/heterotrophic denitrification). Further advantages can be achieved if granular sludge technology is adopted: (i) effective retention of the slow-growing biomass; (ii) superior sludge settleability properties; (iii)

optimization of the microbial community composition. Nevertheless, AMX full-scale implementation worldwide is still limited [1], despite the astonishing attention that the research field has devoted to the novel process in the last decades. Among the obstacles hindering the widespread application of the AMX process there is the long start-up time required by the slow-growing biomass [2]. Seeding with a selected inoculum is a successful solution to achieve rapid start-up or reactor rescue in case of unexpected failures and long-term biomass storage is a key issue to ensure biomass availability when needed [2,3].

Moreover, the composition of real wastewater can impact the long-term stability of granular AMX systems, either due to unbalanced nutrients and/or ions concentrations or for the presence of potential inhibitory compounds. When AMX granular technology is applied to streams prone to mineral precipitation, such as anaerobic digestion

* Corresponding author.

E-mail address: cecilia.polizzi@unifi.it (C. Polizzi).

<https://doi.org/10.1016/j.jece.2021.107002>

Received 10 September 2021; Received in revised form 7 December 2021; Accepted 10 December 2021

Available online 14 December 2021

2213-3437/© 2021 Elsevier Ltd. All rights reserved.

supernatant, landfill leachate or in wastewater reuse systems, the implications of mineral formation on process performance and stability should be carefully assessed and controlled [4,5]. Mineral precipitation has been reported to occur in granular biomass systems, either in anaerobic digestion (AD), partial-nitritation/anammox (PN/A), anammox (AMX) and aerobic granular sludge (AGS), both in lab-scale as well as in real-scale applications [4,6,7]. Precipitate formation strongly depends on influent composition and operational/process conditions such as pH and process influence on pH. Yet, two types of minerals are mainly reported: carbonated minerals and phosphate-bonded minerals; the presence of metal ions, such as calcium and magnesium, is also crucial. Specific pre-treatments or operation strategies are recommended when dealing with wastewaters rich in Calcium (Ca) or Magnesium (Mg), e.g.: (i) preliminary unit for mineral precipitation [8] (ii) membrane filtration [9]; (iii) enhanced formation of inert-rich granules and their consequent withdrawal [7]. As a matter of fact, enhanced Ca-P mineral precipitations in granular biomass has received growing attention for simultaneous N removal and P recovery in anammox granular sludge [7, 10].

According to other works reported in the literature, the positive or negative impact of mineral precipitation on granular biomass depends on the amount of the inert formation, as well as its composition and location [6,11]. From the one hand, mineral precipitation allows for better settleability, higher density and improved mechanical strength of granules [6]. Also, the common phenomenon of granule floatation, and consequent biomass washout, is reported to be effectively reduced in case of controlled P-precipitate formation in the AMX granules [12]. From the other hand, excessive inert concentration would be detrimental due to possible substrate diffusion limitation, reduction of active biomass sites and, ultimately, to granule or granular bed complete mineralization [11]. Indeed, uncontrolled inert accumulation in granular sludge and consequent loss of biomass activity are important factors often overlooked in real plants.

In the present work, a gas lift reactor was inoculated with PN/A granular biomass after more than one-year storage and synthetic influent rich in Ca and inorganic carbon was fed during three out of nine months of operation. The first objective of the present work was to challenge fast reactor start-up with the long-term stored biomass. Then, the issue of mineral precipitation was addressed with the objective of investigating the mechanisms that lead to a severe mineral formation and evaluating the effect on process performance, granules morphology, biomass activity and microbial composition. To the best of our knowledge, this is the first study providing an integrated evaluation of long-term exposure to precipitation-prone wastewaters in an anammox granular reactors, encompassing nitrogen removal efficiency, biomass activity, precipitation characterization and microbial community monitoring.

2. Materials and methods

2.1. Gas-lift reactor

A 7-liter up-flow gas-lift reactor was run for more than 270 days. Fig. 1 presents a schematic of the reactor. Internal gas recirculation was accomplished by a vacuum pump providing a flowrate of around 1 l/min. Reactor headspace was maintained at a slight overpressure of 0.05 bar, visually checked by a pressure-control water lock. A mixture of N₂ and CO₂ (95% and 5%, respectively) was provided manually every day (except weekends), at a flowrate of 0.1 l/min for 20 min. Influent was provided by a peristaltic pump. A U-shape tube was placed prior to the effluent collection tank and acted as a settling control unit. Temperature, pH and ORP were monitored by two probes (5336 T Hach Lange for pH and T; 5361 Hach Lange for ORP). Apart from exceptional events, pH was around 8.1–8.4 and no online pH control was implemented. Temperature was maintained at 30 ± 2 °C, by mean of continuous tempered water recirculation in reactor's jacket. HRT was maintained at 1.1 d for

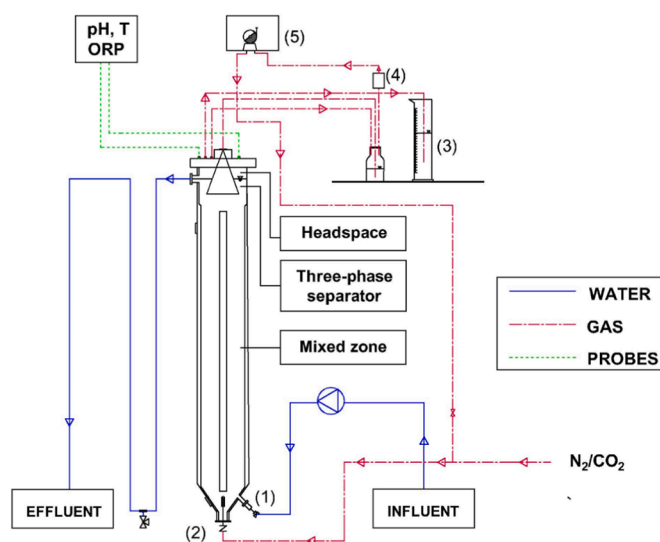


Fig. 1. Experimental set-up. Water line (blue), gas line (dashed red) and sensors (dotted green). Influent port (1); gas recirculation inlet (2); water-lock and overpressure control (3); moisture trap (4); vacuum pump (5).

the first 40 d period, and then increased to 1.6 d from day 41 on. The experimental set-up and the consequent laboratory activities were carried out in the laboratory facilities of the tannery wastewater treatment plant, WWTP (Conorzio Cuoiodepur S.p.a., Pisa, Italy).

Nitrite and Ammonium concentrations in the synthetic influent [13] were set according to the experimental phases and added as NaNO₂ and NH₄HCO₃ or (NH₄)₂SO₄. Distilled water was used for the preparation of the mineral medium, except for the period from day 55–135, during which tap water was used instead. Tap water was non-potable water used in Cuoiodepur WWTP for process operations and was characterised by the following concentrations of the investigated ions: 133 ± 18 mgCa²⁺/l, 45 ± 6 mgMg²⁺/l; 129 ± 18 mgNa⁺/l; 0.067 ± 0.003 mgP/l. Besides, total alkalinity resulted in 440 ppm as CaCO₃; total and carbonate hardness above 44.5 and 36 °F, respectively, denoting that it was very hard water (i.e. water rich in Ca²⁺, Mg²⁺ and HCO₃⁻).

The reactor was inoculated with 500 ml of settled granular biomass from the PN/A plant in Olburgen WWTP, the Netherlands [14]. Initial volatile suspended solid (VSS) concentration in the reactor was about 2.5 gVSS/l. Prior to seeding, the inoculum biomass was kept at 4 °C for 13 months, ensuring a minimum bulk concentration of 100 mgN-NO₃⁻/l, with check on pH and conductivity every 10 days. Regular mixing was provided manually and supernatant was partially renewed with fresh water or nutrient-free mineral medium, when pH and conductivity showed increase higher than 0.5 and 0.5 mS/cm, respectively.

Nitrogen species (ammonium, nitrite and nitrate) were monitored daily, except during weekends. Total and volatile suspended solids (TSS and VSS) were characterized every other week by withdrawing samples from the mixed zone. Also, concomitant TSS and VSS characterization of solids retained in the U-shaped effluent tube was performed. Solids retained in the U-tube were removed from the system, apart from specific cases of intense granule floatation and washout, during which granules were re-introduced in the system. No other active SRT control was performed and SRT was estimated in the range of 200–300 d.

2.2. Experimental phases

Four experimental phases are presented and described in Table 1. Throughout the experiment, influent ammonium/nitrite ratio was maintained at least at the stoichiometric value and, more frequently, slightly above operating under nitrite-limiting conditions. Phase 1 (P1, days 1–15) aimed at biomass reactivation and reactor start-up;

Table 1Applied conditions during the experimental phases. NLR is expressed as N-NO_2^- and inorganic carbon, IC, as C-HCO_3^{2-} .

Experimental Phases (operational days)	HRT [d]	NLR [gN/l/d]	$\text{NH}_4^+/\text{NO}_2^-$ [-]	Ca^{2+} [mg/l]	Mg^{2+} [mg/l]	IC [mg/l]	P_{tot} [mg/l]
P1-start up (1–15)	1.1 ± 0.3	0.02–0.09	2.3 ± 0.3	54	10	224 ± 61	5
P2- NLR increase (16–130)	1.1–1.6 ^b	0.09–0.50	1.0 ± 0.1	132 ± 94	36	498 ± 334	5
P3 – Process disruption (131–154)	1.6 ± 0.2	0.50 ± 0.05	0.8 ± 0.1	83 ± 94	55	643 ± 124	5
Off-site biomass rescue (155–177)	–	–	–	–	–	–	–
P4- Process restoration (178–270)	1.6 ± 0.2	0.22 ± 0.02	0.9 ± 0.1	–	10	57	5

^a Reference stoichiometric $\text{NH}_4^+/\text{NO}_2^-$ ratio is considered 0.9 [16].

^b HRT was set at 1.1 d from day 15 to day 40. Then increased to 1.6 d from day 41 on.

ammonium and nitrite inlet concentration were 100–200 $\text{mgN-NH}_4^+/\text{l}$ and 45–200 $\text{mgN-NO}_2^-/\text{l}$, respectively, with a weekly stepwise increase of 50 mgN/l for nitrite. An inlet concentration of 150 $\text{mgN-NO}_3^-/\text{l}$ was dosed as redox buffer. Also, 10 mgCOD/l as acetate were added to restore glycogen storage that might have been consumed due to one-year starvation [15]. The aim of Phase 2 (P2, days 16–130) was to maximise the reactor removal capacity by progressively increase inlet concentration, i.e. inlet load. As a general rule, influent concentration increase was applied when effluent nitrite concentration showed a decreasing trend for at least three consecutive days or when it kept stably below 10 $\text{mgN-NO}_2^-/\text{l}$. In a few cases, nitrite accumulation raised up to 100 $\text{mgN-NO}_2^-/\text{l}$. At the occurrence of these events, the feeding was paused and the reactor was operated in batch condition until nitrite concentration decreased to less than 40 $\text{mgN-NO}_2^-/\text{l}$. Phase 3, (P3, days 131–154), was characterized by intense mineral precipitation on the granules' surface and concomitant process instability and deterioration. Severe increase of nitrite concentration was observed together with a change in granules appearance. An off-site rescue procedure was implemented during days 155–177 as described in Section 3.1 (not reported in process performance graphs). Process stability was restored in phase 4 (P4, days 178–270) at a NLR of 0.22 $\text{gN-NO}_2^-/\text{l/d}$. The main hardness-related components in the feeding medium, resulting from salt addition in distilled or tap water, are also presented as average values in Table 1.

The off-site rescue procedure was as follow: (i) gravimetric selection was applied exploiting the high density of mineral-covered granules; (ii) granules characterised by severe precipitation and higher density were removed from the system; (iii) the remaining biomass was re-suspended in HEPES-buffered medium at pH 6.5 for five consecutive days, replacing the slightly acid medium every day, in order to dissolve residual carbonate minerals as much as possible.

As ammonium was intentionally dosed in excess (nitrite-limiting conditions), Nitrogen Loading Rate (NLR), Nitrogen Removal Rate (NRR) and Specific Nitrogen Loading Rate (SNLR) were referred to the sole nitrogen-nitrite. Total nitrogen (TN) removal rate is also presented and refers to the sum of inorganic nitrogen species (nitrite, nitrate, ammonium). The SNLR was calculated as the applied NLR specific for the VSS content of the reactor. General stoichiometry was checked by means of mass balances on the nitrogen compounds.

2.3. Activity batch tests

Two types of activity batch tests were performed: in-situ tests and manometric tests. In-situ tests were conducted by operating the reactor in batch-mode. In case of nitrite accumulation (above 80 $\text{mgN-NO}_2^-/\text{l}$), the inlet was stopped, the reactor was operated in batch-mode and samples were collected every 45 or 120 min to assess the maximum removal capacity of the reactor (NRR_{max} , gN/l/d). Manometric tests were conducted in 300-ml Oxitop® bottles, similarly to the procedure adopted by Lotti et al. [17]. Fresh biomass was withdrawn from the mixed zone of the reactor and re-suspended in nutrient-free mineral medium. A mixture of N_2/CO_2 (95% and 5%, respectively) was sparged in the headspace to ensure anoxic conditions. Bottles were placed in a pre-heated incubator at 30 °C. Continuous mixing was provided by an

orbital shaker set at 180 rpm. Concentrated pulses of 1 M $(\text{NH}_4)_2\text{SO}_4$ and 1 M NaNO_2 solutions were spiked in order to provide 30–80 mgN/l , as nitrite and ammonium, in the liquid phase. A minimum $\text{NH}_4^+/\text{NO}_2^-$ ratio of 1 was ensured. When N_2 exponential production phase was followed by stable pressure plateau, a further pulse of concentrated solutions was provided. In each test, a minimum of three and a maximum of five consecutive spikes were provided in order to have a more robust estimation of the maximum activity. After each test, the total amount of biomass was used for VSS assessment. On average, biomass concentration ranged from 0.6 to 1.2 gVSS/l .

Manometric tests allowed to assess the maximum specific anammox activity (MSAA), expressed as gN/gVSS/d , whereas the in-situ batch tests allowed the estimation of the maximum removal capacity of the reactor (NRR_{max} , gN/l/d). These two data were matched with the reactor VSS concentration in order to be straightforwardly comparable. A total of 10 activity tests were performed. As above, due to the applied nitrite-limiting condition, MSAA and SNLR were referred to the sole nitrogen-nitrite [18].

2.4. Analytical methods

Ammonium, nitrite and nitrate were measured spectrophotometrically, using commercial kits (Dr Hach Lange). VSS and TSS were assessed in triplicate, according to standard methods [19] and their determination was not affected by precipitate formation. The following parameters were analysed on tap water: (i) Ca^{2+} , K^+ , Mg^{2+} , Na^+ by ionic chromatography (UNI EN ISO 14911:200, from an external laboratory); (ii) total alkalinity according to Italian standard regulations (method 2010 B APAT and IRSA CNR [20], from an external laboratory) and metals and total phosphorous by Inductively Coupled Plasma Optical Emission Spectrometry, ICP-OES (Optima 2100 DV ICP-OES, PerkinElmer). Acid tests were performed on the inert formation by applying a few drops of 1 M HCl in order to assess the presence of carbonate-related minerals. Acid test is commonly used in geology to identify carbonates minerals, comprising mineral compounds of CO_3^- ions with metals, since acid addition dissolves the minerals by turning carbonates into gaseous CO_2 [21,22]. Also, qualitative assessment of total and carbonate-related hardness was obtained through commercial Quantofix® test strips.

2.5. Microbial community analysis, granular size distribution and electron microscopy analyses

Biomass samples were collected every 30–45 days for Next Generation Sequencing (NGS) analyses. Genomic DNA was prepared from 250 mg sludge pellet obtained from 10k rpm centrifugation in an Eppendorf MiniSpin Plus, using Qiagen PowerFecal(R) Pro DNA kit according to manufacturer instructions. DNA concentration and purity was checked by NanoDrop ND-1000 (Thermo Fisher Scientific) and 1.5% agarose (TopVision, ThermoFisher Scientific) gel electrophoresis (run 30' at 90 V on a MiniSub Cell GT system, BioRad) stained with SYBR Safe DNA Gel Stain [23]. Primers couple from Takahashi et al. [24], with a slightly modified forward primer, optimised for anammox bacteria were used for PCR amplification of the V3 and V4 variable regions of the 16 S rRNA, gene as reported in [23]. Amplicons were then sent to an external

laboratory (BMR Genomics, Padua, Italy) and sequenced in paired-end (2×300 cycles) on the Illumina MiSeq platform. For Operational Taxonomic Units (OTU) analysis reads were processed using the MICCA pipeline. Additional information is available in Niccolai et al. [25].

Granular size analyses were performed by mean of image elaboration through the software Image ProPlus® [26]. SEM-EDX and TEM analyses were performed on a dozen of granules in order to study their superficial appearance and composition as well as the internal structure. For SEM-EDX samples preparation, an overnight fixation with 2.5% glutaraldehyde and 0,1 M BPS was conducted; then, repeated rinsing with the same BPS were performed prior to dehydration at increasing ethanol concentrations (50–100%) and, subsequently, at hexamethyldisilazane (HMDS). Dried samples were coated with Gold and Platinum, prior to their analysis. For TEM sample preparation, fixation was performed in glutaraldehyde and osmium tetroxide according to the procedure by Lin and Wang [27]; samples were then embedded in

Epon-araldite resin, sectioned with an RMC PowerTome X ultra-microtome and stained with uranyl acetate and lead citrate. TEM observations were conducted with a JEOL JEM-100SX electron microscope.

2.6. Mineral formation simulation

The software Visual MINTEQ 3.1 [28] was used to calculate the saturation index of each possible compound, according to the maximum ions concentrations applied (Table 1), pH and temperature conditions. Saturation Index is expressed as:

$$SI = \log \frac{IAP}{K_{ps}}$$

where IAP is the Ionic Activity Product and K_{ps} is the solubility product of a given compound [7]. SI values higher than 0 indicate super

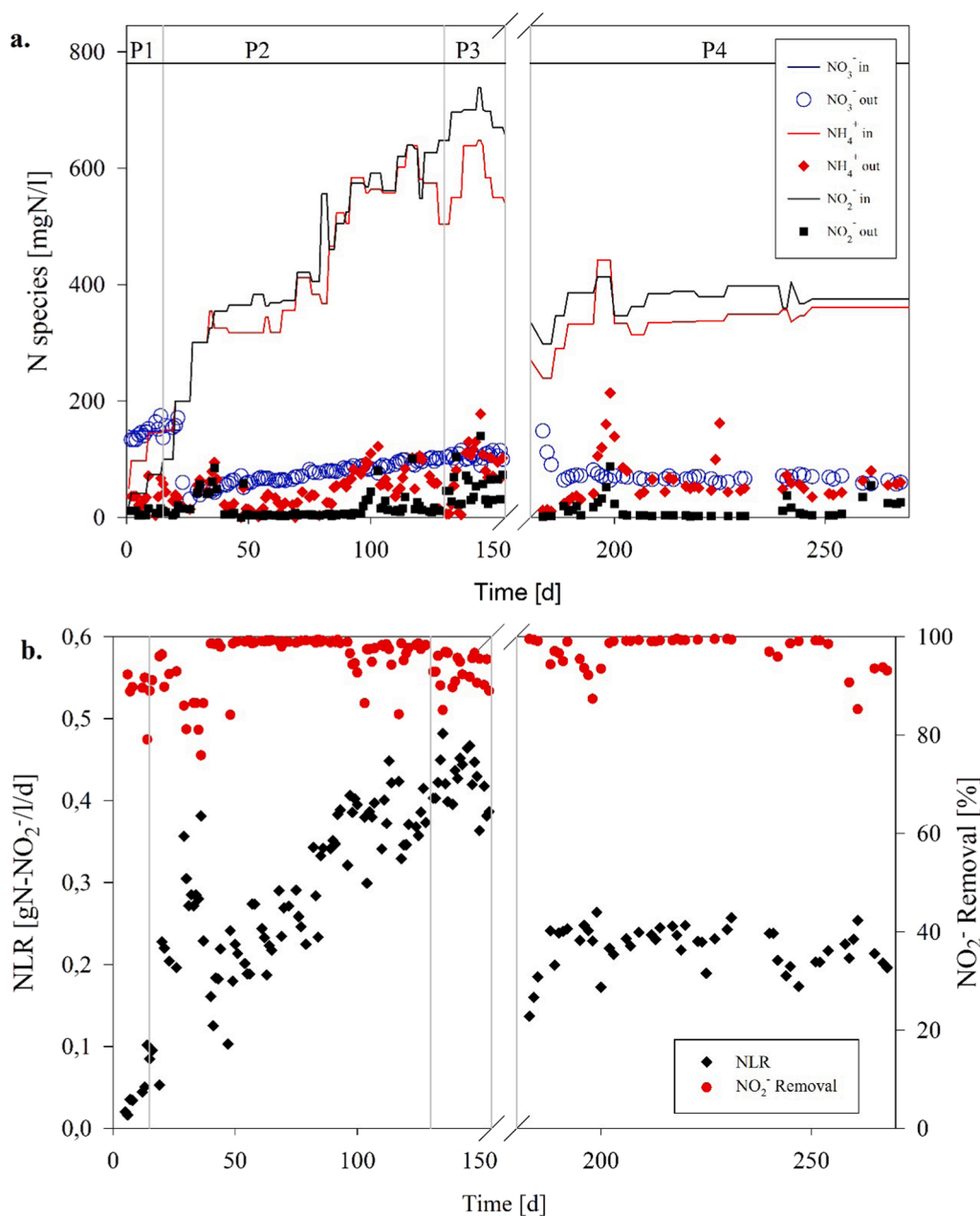


Fig. 2. Influent and effluent nitrogen concentration (a); NLR and NO_2^- removal efficiency (b). Nitrate was dosed in phase 1 only, at influent concentration of 150 mgN- NO_3^- /l.

saturation conditions, i.e. the possibility of precipitation. The condition with the highest nitrogen load was considered (upper limits of ions concentration ranges, Table 1), as a worst-case scenario.

3. Results and discussion

3.1. Reactor operation

Reactivation phase P1 was relatively fast as noticeable nitrite and ammonium removal was observed after the first two weeks of operation (Fig. 2a). Nitrite effluent concentration stayed below $10 \text{ mgN-NO}_2^-/\text{l}$, and a proportional nitrate increase was shown as well, indicating active growth of anammox bacteria [16]. Since the concept of *reactivation* is not absolute, in the present work, reactivation refers to the positive response of the biomass to the applied nutrient load, i.e. no nutrients were accumulated in the effluent. During P2, the relatively high pace in influent nitrogen concentration (75% NLR increase in less than 10 days) lead to nitrite accumulation up to $80 \text{ mgN-NO}_2^-/\text{l}$, on day 37. On this day, inflow was paused and an in-situ activity tests performed (see Section 3.2). Results showed that the applied NLR was above the NRR_{max} of the system (0.30 vs $0.23 \text{ mgN-NO}_2^-/\text{l/d}$, applied NLR vs NRR_{max} , respectively). Moreover, granules flotation was observed in those days and biomass washout was likely contributing to process instability. Granules flotation has been reported by many authors as related to system overloading and consequent nutrient accumulation in the bulk as some of the major causes [18,29,30]. Indeed, granules flotation was observed when bulk NO_2^- concentration was around $80\text{--}100 \text{ mgN/l}$. Consequently, NLR was lowered by decreasing the flowrate from 7 to 4 l/d. The resulting 1.6-day HRT was kept from this day on. From day 35–70 stable operation was maintained to avoid overload conditions. After this period, nitrite removal efficiency was constantly higher than 95% (Fig. 2b) and the biomass appeared with a bright carmine colour, smaller in size and with a more uniform granular dimension (see Section 3.3). NLR increase strategy was started again on day 71. Until day 90, the reactor responded positively to almost 40% increase in NLR ($0.35 \text{ mgN-NO}_2^-/\text{l/d}$), with stable nitrite effluent concentration around at $4 \pm 1 \text{ mgN/l}$. Since day 90 to day 120, the reactor stood NLR up to $0.48 \text{ mgN-NO}_2^-/\text{l/d}$ (0.1 gTN/l/d) but a slight but progressive process disruption was observed together with an increase in pH (up to 8.9) and decrease in VSS/TSS ratio. Regular episodes of nitrite (and ammonium) accumulation occurred and resulted in concentrations up to 80 and $102 \text{ mgN-NO}_2^-/\text{l}$ on day 103 and 117, respectively (Fig. 2a). Nitrite accumulation showed chronic after day 130, despite contingent measures as the reduction of influent nitrite concentration (days 120–130).

Reactor solids monitoring revealed that, beside a gradual increase in the overall VSS concentration, a dramatic decrease in VSS/TSS ratio was

observed from day 60 to day 140, as shown in Fig. 3. On day 83, a VSS/TSS ratio decreased by around 30% and the VSS/TSS decreasing rate remained almost linear until day 140, when the lowest VSS/TSS ratio (35%) was registered. Concomitant changes in granule appearance and density were observed: granules progressively turned from bright red to whitish and their density increased notably, since usual agitation provided by gas flow recirculation was not sufficient to suspend the biomass, which started to settle at the bottom of the reactor. Further evidences, discussed in Section 3.4, showed that the increase in the non-volatile fraction of TSS (NVSS) was mainly due to a mineral deposition on the surface of the granules after three-month feeding with hard tap water, as presented in Table 1 and Fig. 3. Acid tests on granules' mineral ash indicated that the minerals had a high carbonate content as the characteristic fizzing was observed.

On day 155, the reactor was emptied, and an off-site rescue strategy was implemented with the aim of removing granules severely affected by mineral precipitation. As a fact, precipitation did not affect all the granules at the same extent. Fig. 4a shows the macroscopic appearance of the granules affected by severe mineral deposition and their inorganic shell after incineration at 550°C . Granules ash looked like whitish mineral shell around the granules.

At the end of phase 3, some granules appeared completely covered of a whitish shell whereas others appeared almost free from any deposition (Fig. 4a). The rescue procedure described in Section 2.2 was adopted.

The rescued biomass was almost half of the total biomass present in the reactor during the reference period of days 130–150 and was inoculated back in the reactor on day 178 (restoring phase, P4). An in-situ activity test was performed in order to set the proper NLR according to the system capacity. In order to promote the residual carbonates dissolution, a Calcium-free synthetic medium was prepared, NaHCO_3 was dosed at 400 mg/l and influent pH was lowered to 6.5. Taking into account that the biomass was halved and underwent critical conditions, a 60% reduced NLR was applied. From day 200 on, stable NLR of $0.22 \text{ gN-NO}_2^-/\text{l/d}$ (0.47 gTN/l/d) was applied at HRT of 1.6 d, and a stable 95% nitrite removal efficiency was established.

Table 2 shows the observed stoichiometry throughout the experimental phases as $\text{gN-NO}_2^-_{\text{removed}}/\text{gN-NH}_4^+_{\text{removed}}$ and $\text{gN-NO}_3^-_{\text{produced}}/\text{gN-NH}_4^+_{\text{removed}}$. Results were in agreement with the stoichiometry reported by Lotti et al. [16]. A slight increase in both N ratios were observed during the most critical periods (P3 and first days of P4). It can be speculated that an additional ammonium release could be derived from cellular lysis (ammonification) in the inner layers, thereby affecting the measured ratios.

3.2. Activity tests

Manometric and in-situ batch tests showed comparable results when both types of tests were performed within a few days, corroborating the applied stoichiometry as well as the reliability of the methods (Fig. 5). On day 36 and 47 the MSAA was $0.155 \pm 0.004 \text{ gN-NO}_2^-/\text{gVSS/d}$, considering results from both types of test, and it more than doubled after one month, reaching $0.349 \pm 0.034 \text{ gN-NO}_2^-/\text{gVSS/d}$, on day 83, confirming the successful biomass reactivation and the fast reactor start-up. The progressive process disruption and VSS/TSS decrease observed in the reactor was reflected in a decline in MSAA on days 117 and 135, with a decrease of the 21% and 59%, respectively, compared to the maximum value observed on day 83. The lowest MSAA of $0.279 \pm 0.035 \text{ gN-NO}_2^-/\text{gVSS/d}$ was detected on day 135 in correspondence of the lowest VSS/TSS ratio observed. Successful process restoration after biomass rescue and segregation, lead to VSS/TSS restoration around 90% and a corresponding increase of the MSAA on day 178 (after re-inoculation) was observed up to its maximum value of $0.387 \pm 0.027 \text{ gN-NO}_2^-/\text{gVSS/d}$ on day 218, maintained quite stable also on day 245. In Fig. 5, the SLNR is also plotted. On days 35, 47 and 135 the SLNR was higher than the MSAA of the biomass; consistently, nitrite accumulation was observed in those days. In phase 4 (days 218 and 245), as the MSAA

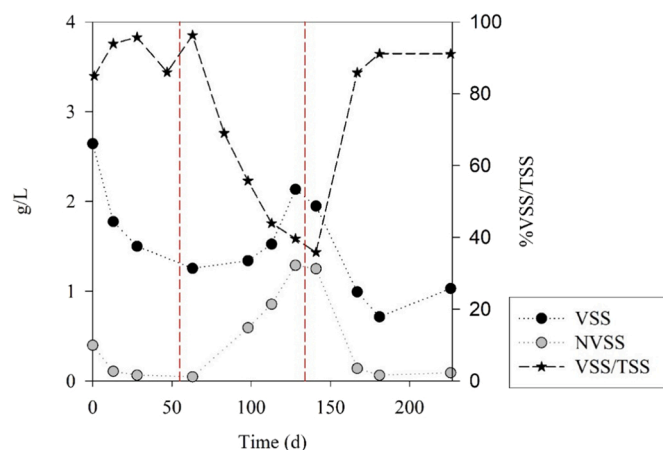


Fig. 3. VSS concentration in the reactor and VSS/TSS ratio. Dotted vertical lines define the hard-water feeding period.

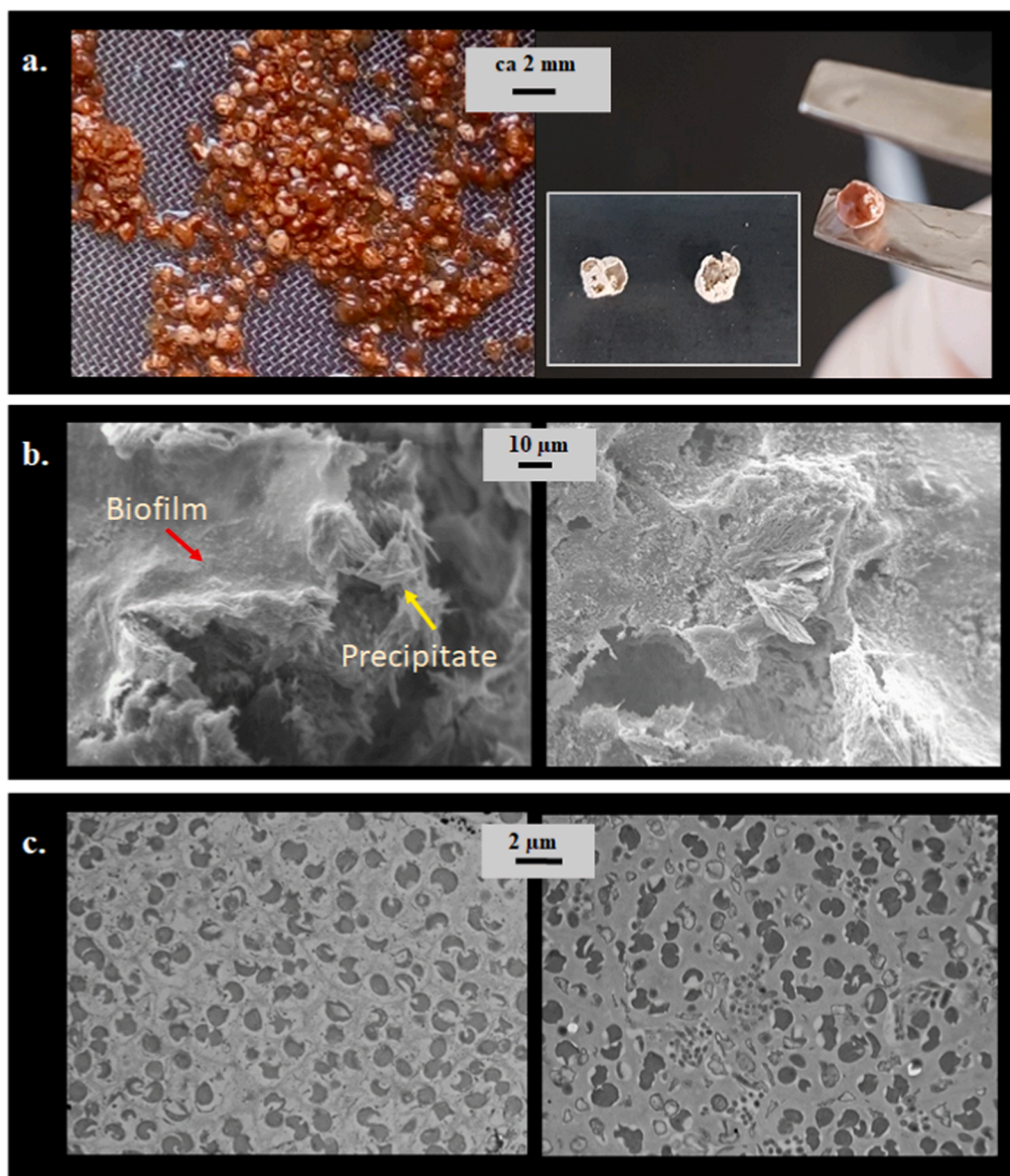


Fig. 4. Pictures of anammox granular biomass on day 155: on a 0.5-mm sieve on the left and after incineration at 550° on the right (a). SEM images of a granules showing evident mineral precipitation exhibiting two types of surfaces: a biofilm-like uniform layer over a rough irregular surface with crystal precipitates (b). TEM observations on sections of granules not affected by mineral precipitation on the left, withdrawn in phase 4, and with evident precipitation on the right, withdrawn in phase 3 (c).

Table 2
Observed stoichiometry during the operational phases.

Phase	Days	$\text{NO}_2^-/\text{NH}_4^+$ [gN/gN]	$\text{NO}_3^-/\text{NH}_4^+$ [gN/gN]
P1-start up	1–15	–	–
P2- NLR increase	15–130	1.146 ± 0.080	0.167 ± 0.063
P3 – Process disruption	131–155	1.271 ± 0.045	0.165 ± 0.008
Off-site biomass rescue	155–177	–	–
P4- Process restoration	178–225	1.322 ± 0.092	0.211 ± 0.072
	226–270	1.182 ± 0.091	0.164 ± 0.058

raised again to the highest values observed on day 83, the constant SNLR applied ranged 60–65% of reactor's maximum capacity.

3.3. Microbial community and granular size distribution

Size distribution analyses were performed on the inoculum biomass and on day 40 and 260, representative of phase 2 and phase 4,

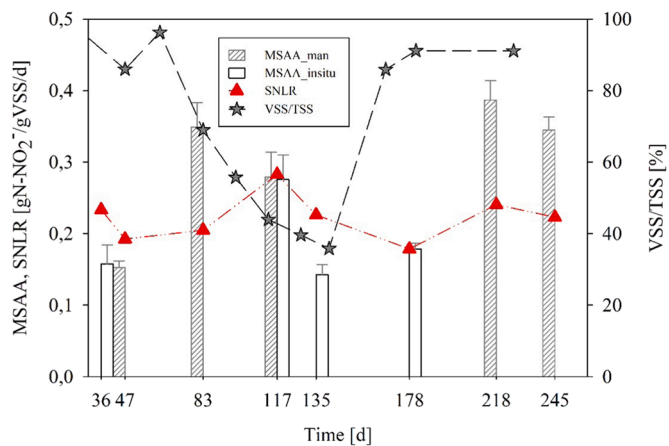


Fig. 5. Results on activity tests versus the applied SNLR and the observed VSS/TSS ratio. MSAA from manometric assays (black columns) and from in-situ batch tests (white column), as average and standard deviation values.

respectively, as well as on floating granules collected during severe floating events on days 40–50. After 40 days of operation, granules' average diameter was 1.11 mm, lower than the one of the inoculated sludge (1.55 mm). A higher average diameter of 1.82 mm was observed on day 260 (P4, after process restoration), when the diameter values falling in the 10th, 50th and 100th percentile were much closer among each other in comparison with those of previous samples, witnessing higher homogeneity in granular size distribution. The most abundant granulometric classes were 0.5–1 mm and 1.1–1.5 mm on days 40 and 260, respectively. Floating granules exhibited by far the highest average diameter of around 3 mm, in agreement with other works (Chen et al., 2010; Dapena-mora et al., 2004). As reported by Chen et al. [31], AMX granular size below 2.2 mm is recommended to control granule floatation, whereas particle size of 1.5 and 2.0 mm are suggested to be selected to maintain high and stable nitrogen removal. The average granular size of 1.5 and 1.8 mm obtained in the stable period of phase 2 and 4 are in line with the above recommended range and nitrogen removal performance was, in fact, high and stable.

In Fig. 6, the microbial distribution in terms of relative abundance is presented at class (a) and genus level (b), for each of the experimental

phases. Days 49, 105 and 290 are representative of phase 2, 3 and 4, respectively. Day 190 falls at the beginning of phase 4, two weeks after biomass re-inoculation. *Planctomycetia* was the class showing the highest relative abundance in all the samples, whose percentage remained almost constant throughout the experimental phases, namely $38 \pm 3\%$. At genus level, anammox bacteria were related to "*Candidatus Brocadia*" and "*Candidatus Kuenenia*" and an interesting population change within them was observed. "*Ca. Brocadia*" was the predominant planctomycetes on days 49, 105 and 232 with relative abundance of 38%, 35% and 25%. Only the sample on day 190 showed a significantly lower relative abundance (15%) in "*Ca. Brocadia*". A complementary behaviour was observed for "*Ca. Kuenenia*" which was almost absent on day 49, but its relative abundance achieved 5% and 19% on day 105 and 190, respectively, and decreased to 8% on day 232. On day 49 (Phase 2), the reactor was responding very well to the fast increase in NLR, whereas on day 190 process deterioration was evident due to the intense precipitation.

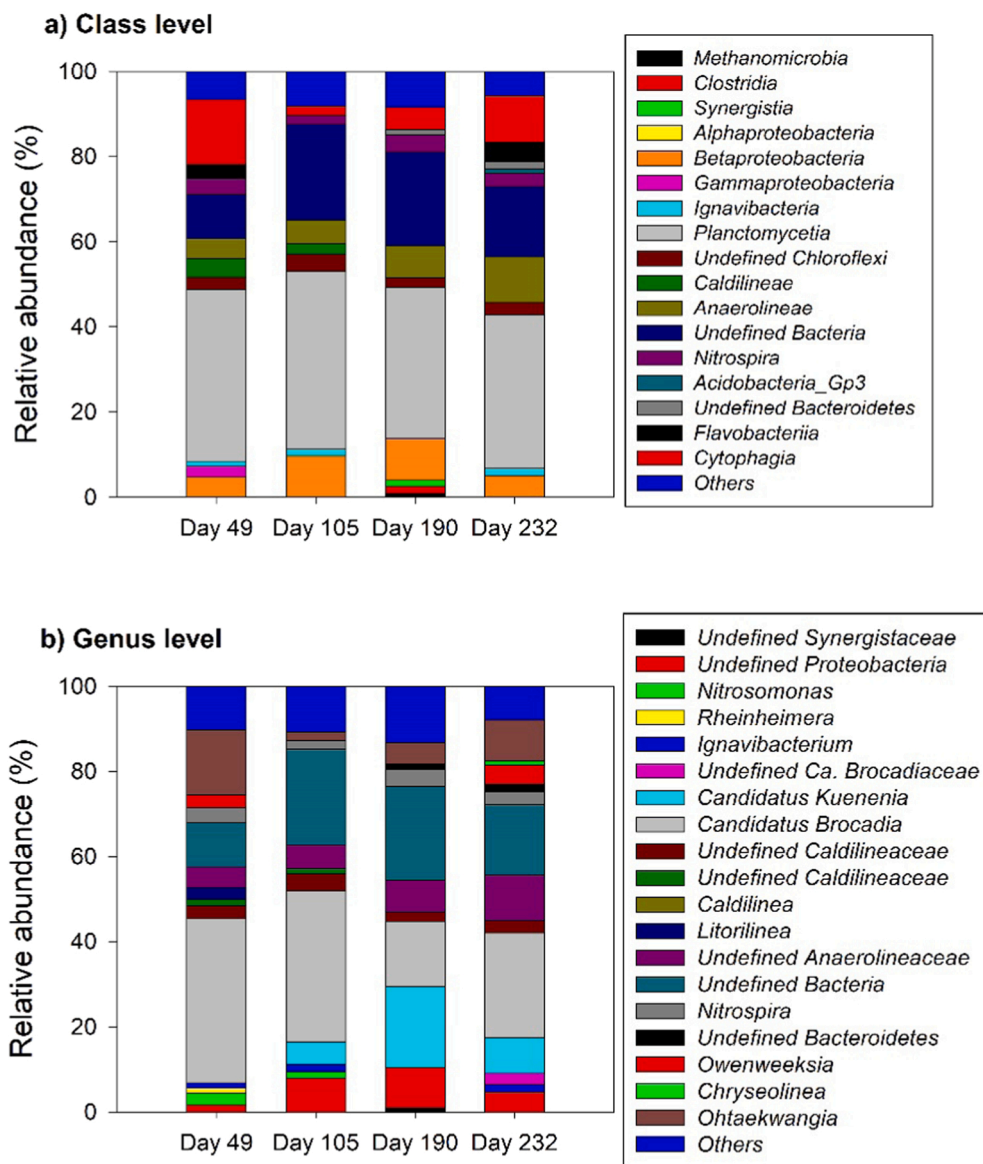


Fig. 6. Microbial diversity profiles over the experimental work, at class (a) and genus level (b). Only Operational Taxonomic Units with relative abundance higher than 1% are displayed.

3.4. Mineral formation mechanism and discussion

Software Visual Minteq 3.1 prediction on mineral precipitation were: (i) calcite, around 2 mM; (ii) dolomite, around 2 mM and, in a little extent (iii) hydroxyapatite, around 10^{-2} mM. ICP-OS analysis carried out on tap water and effluent samples (on days 140 and 180), shows values of 0.07 ± 0.01 and 3.77 ± 1.1 mgP_{tot}/l, respectively. Since influent P- PO₄³⁻ was dosed at around 5 mg/l, the total P concentration in reactor effluent witnesses that the majority of P-PO₄³⁻ was exiting the system, net of biomass uptake and possible marginal precipitation, confirming the hypothesis that the visible mineral precipitate was not belonging to any of the Ca-PO₄ bonded minerals. This was likely due to the fact that influent PO₄³⁻ concentration was kept as low as 5 mgP/l throughout the experimental phases. The ions concentrations applied throughout phase 2 were such to determine the severe inert formation observed at the beginning of phase 3. Even though Ca, Mg and IC concentrations were lowered in phase 3 (distilled water was used after day 135), no positive effect was observed. Bicarbonate concentration in phase 4 showed sufficient for the anammox IC requirement while preventing any further precipitation drawback. The calcium concentration observed in the present study is within the range of 40–600 mg/l that is reported to promote anaerobic sludge granulation [32] and even higher concentration can be found in landfill leachate and industrial wastewaters where lime is used as buffering agent [4]. Intense mineral formation is pointed as an important warning for real-scale treatment of such streams, whose concentration and saturation conditions could be comparable to those reported in the present work.

As presented in Fig. 4b, SEM-EDX analysis showed that the general morphological appearance of the granules exhibited the typical cauliflower-like aspect with concavities and irregular pattern [33,34]. Average O/C molar ratio was calculated over the spectrum analyses in 8 internal and three external points on a precipitate-free granule and resulted in a 0.56 ± 0.19 , slightly higher than the value of anammox biomass composition of CH_{1.74}O_{0.31}N_{0.20} [16], more in line with the O fraction in the general formulation of biomass CH_{1.8}O_{0.5}N_{0.2} [35]. Biomass composition by Lotti et al. [16] was estimated from an almost pure culture of free-living anammox cells, a condition far different from the one of the present study, with granular sludge (EPS-rich VSS) with an almost complete sludge retention. Calcium fraction results in negligible concentration (below 5% in weight) in precipitate-free granules. SEM images on granules with evident mineral precipitation allow to distinguish a thin uniform surface reminding to biofilm aggregates and a more irregular and rough surface reminding inorganic structures (Fig. 4b). EDX analyses revealed that Ca was much more abundant in the irregular surface, compared to the biofilm-like one. Phosphorus was not detected in any of the analysed areas, confirming that the inert precipitation was not related to phosphate-bond minerals. No other relevant elements were detected (concentrations below sensitivity threshold of the instrument). EDX analyses over several points and areas of surfaces with precipitate-like appearance returned a Ca/C molar ratio ranging from 0.9 to 2.5, confirming that the mineral was CaCO₃-like as predicted by the saturation indexes. The higher values observed suggest either that others Ca-based minerals were present, or that the results on the analysed areas were affected by biofilm aggregates interference (not-clearly distinguishable). TEM analyses showed that granules not affected by precipitation (withdrawn in phase 4) showed a dense presence of the typically round shaped anammox, with the usual concavity on the cellular wall (Fig. 4c). A tertiary organization in AMX granules' structure with a first level of aggregation among few cells (clusters or zoogloae), a secondary aggregation embedded by EPS and a tertiary cementation of aggregates has been proposed by Lin et al. [27] and Kang et al. [34]. Such a sub-unit structure is clearly represented for granules free from precipitation, where microorganisms other than AMX were detected in the interspaces among (and not within) bacteria agglomerates. A lower resolution was obtained in samples affected by significant precipitations, probably due to a lower efficiency in the preliminary

fixation procedure, possibly related to limited diffusion of reactants due to the mineral shells. As a general consideration for precipitate-affected granules, AMX cells appear more dispersed and non-anammox micro-organism are encountered more randomly over the analysed areas. Similar evidences were reported by Hu et al. [36], comparing anammox granules grown under nutrient abundance (dense cell agglomeration) vs nutrient limitation (dispersed cell distribution). In the present work, it is, in fact, assumed that mineral precipitation lead to nutrient diffusion limitation along the granule section, as discussed below.

The location of mineral precipitation is also of interest. Most of previous works report precipitation as occurring in the core of the granule, and several reasons have been proposed to support this evidence. First, mineral precipitate nuclei can form in the bulk liquid and may act as supporting material for granule formation; then, the inner region of the granule is typically less active, with a higher pH and more abundant in inert cellular-lysis product and minerals, compared to the external layers. Undesired carbonates precipitation into AMX granules has been reported recently by Ma et al. [7], during the operation of enhanced precipitation of hydroxyapatite in the bioreactor, at bulk pH of 8.5 or above. In the present study, carbonate precipitation occurred at lower pH, around 8.1; yet, the saturation pH, as defined by Langelier [37], strongly depends on the level of calcium and bicarbonate, the latter being 5–9 times higher in the present work (in phase 2 and 3, respectively) compared to Ma et al. [7]. Precipitation onto the surface of AMX granular biomass seems far more unusual and it has been experienced by Trigo et al. [38] and Zhang et al. [39], both operating AMX systems with synthetic influent and observing undesired apatite-like and calcite-like precipitation, respectively. Substrate diffusion limitation from the bulk to the inner layers may occur in case of surface precipitation [39]. In the present study, a well-defined mineral shell was clearly visible in many granules during phase 2–3, suggesting that substrate diffusion limitation can be ascribed as one of the main mechanisms that lead to progressive process disruption, since the mineral shell can act as physical barrier for substrate diffusion. Insufficient mixing due to higher granule density and biofilm erosion and consequent biomass washout caused by shear stress increase due to hard-particle collision were also considered responsible as cascade effects. Further analyses on sludge volume index and granules density could have been carried out to support these assumptions. In this work, the evidence that the precipitation occurred on the surface of the granules and did not affect other surfaces on the bulk liquid (such as submersed probes or tubes) suggested that the precipitation reaction was somehow locally induced by biological processes [40]. Local pH gradients at the granule surface, due to the proton-consuming AMX activity, are likely to be the major drivers to promote local precipitation offering a favourable surface for incipient calcite precipitation and the consequent deposition. Compared to the studies reported above, it is believed that the higher Ca and IC concentrations of the present work together with local pH gradients in the anammox granules' surfaces triggered surface instead of inner-core precipitation. Moreover, Extracellular Polymeric Substances (EPS) have been reported to present binding functional groups for several metals, including Ca [41,42] and thereby, it can be speculated that the Ca arrangement around the granules could have further favoured granules' surface as preferable nucleation site. Restated, the conditions presented in the present work, mainly related to ions concentration and their interaction with active anammox granules, were such to create conditions favourable to precipitation at the interface between granule surface and the bulk liquid; differently, in studies reporting on nuclei mineralization these favourable conditions were likely existing in the granule core instead.

In this work, we observed that biomass activity was clearly affected by precipitation, since the lowest MSAA was detected at the lowest VSS/TSS ratio and the highest MSAA at the restored VSS/TSS value as high as 90%. These evidences confirm that mineral precipitation had, in fact, a negative impact on biomass activity, in line with other studies [38]. Even though the decreasing trend of VSS/TSS ratio was clear already on

day 83, i.e. after less than one month of hard water feeding, the dramatic effect of mineral precipitation on process stability was not evident until days 130–150 (phase 3), i.e. two months later. Consistently, even though the biomass activity was also facing a progressive decline, nitrite accumulation in the effluent was not observed until reactor nitrogen removal capacity fell below the applied nitrogen loading rate. In real-scale applications, effluent nitrite accumulation is possibly a late warning of process instability. On the contrary, an integrated monitoring of effluent nitrogen concentrations, reactor solids (possibly at different reactor height) and biomass activity can allow for prompt detection of process deterioration.

The changes in population somehow supports the hypothesis of significant substrate diffusion limitation. “*Ca. Brocadia*” is reported to be an r-strategist organism, basing its competitive advantage on high growth rate. On the contrary, “*Ca. Kuenenia*” is reported as k-strategist instead, basing its competitive advantage on high affinity [43]. Under the assumption that severe precipitation hindered substrate diffusion within the granule, substrate-limiting conditions might have resulted in the internal layers, where anammox used to thrive on high substrate concentrations, promoting a (temporary) advantage of “*Ca. Kuenenia*” over “*Ca. Brocadia*”, as observed on day 190, i.e. at the end of the most critical period. In line with such an assumption is the finding that “*Ca. Brocadia*” returned to be the predominant anammox genus as the process stability was restored and the most damaged biomass removed.

In light of all the evidences gathered in the present study, we suggest that case-specific operational strategies should be put in place when treating precipitate-prone wastewaters. A simple but effective strategies, as the one implemented in the present work, comprises a regular VSS/TSS and biomass activity monitoring together with biomass withdrawal (as biomass wastage) from reactors’ bottom in order to prevent severe inert accumulation in the system and limit maintain stable process performance.

4. Conclusions

The present work offers a comprehensive study on the problem of mineral precipitation in anammox granular sludge. The main findings can be summarized as follows:

- A successful biomass reactivation of a long-term stored PN/A granular biomass allowed for a fast reactor start-up and NLR increase, confirming that proper storage of active biomass is a feasible option in case of scarcity of seed sludge.
- Intense precipitation, observed after three months of hard-water feeding, impacted granular sludge morphology and microbial composition.
- Substrate diffusion limitation within the granule is deemed the main mechanisms that lead to biomass activity loss and consequent process deterioration. Such a condition likely provided a temporary advantage of the k-strategist “*Ca. Kuenenia*” genus over the r-strategist “*Ca. Brocadia*”, during the phase with the most severe precipitation.
- The integrated results from chemical analyses, simulated precipitation conditions and SEM-EDX analyses indicated that the inert formations were calcium and carbonate-based, likely to be formed in waters with high calcium and carbonate-related alkalinity.
- Gravimetric selection showed to be an effective solution for discarding granules with excessive precipitation and recover system performance, such a criterion can be applied also in real-scale implementations. Careful monitoring of the VSS/TSS ratio as well as the regular withdrawal of the denser granules from reactor’s bottom are suggested for inert accumulation control.

Supplementary data of this work can be found in online version of the paper.

CRediT authorship contribution statement

C. Polizzi: Conceptualization, Wet laboratory, Supervision, Writing. **T. Lotti:** Conceptualization, Discussion, Supervision. **A. Ricoveri:** Wet laboratory. **R. Campo:** Granulometric analysis. **C. Vannini:** TEM analysis. **M. Ramazzotti:** 16s rRNA NGS data analysis. **D. Gabriel:** Supervision, Discussion, Funding acquisition. **G. Munz:** Supervision, Discussion, Funding acquisition. All the authors contributed to the revision of the work and agreed with the final version of the article.

Declaration of Competing Interest

The authors declare that they have no known competing financial interests or personal relationships that could have appeared to influence the work reported in this paper.

Acknowledgement

The present work was supported by a financial contribution from Consorzio Cuoioepur S.p.a. (Pisa, IT) and was partially developed within the Project Recycles (GA: 872053) funded by the European Commission within the Horizon 2020 Mary Skłodowska Curie Rise 2019 programme.

Appendix A. Supporting information

Supplementary data associated with this article can be found in the online version at [doi:10.1016/j.jece.2021.107002](https://doi.org/10.1016/j.jece.2021.107002).

References

- [1] Y. Xue, H. Ma, Z. Kong, Y. Li, Formation mechanism of hydroxyapatite encapsulation in anammox-HAP coupled granular sludge, *Water Res.* 193 (2021), <https://doi.org/10.1016/j.watres.2021.116861>.
- [2] M. Ali, M. Oshiki, S. Okabe, Simple, rapid and effective preservation and reactivation of anaerobic ammonium oxidizing bacterium “*Candidatus Brocadia sinica*”, *Water Res.* 57 (2014) 215–222, <https://doi.org/10.1016/j.watres.2014.03.036>.
- [3] X. Wang, J. Huang, D. Gao, International Biodeterioration & Biodegradation Effects of three storage conditions on the long-term storage and short-term reactivation performances of anammox granular sludge, *Int. Biodeterior. Biodegrad.* 164 (2021), 105310, <https://doi.org/10.1016/j.ibiod.2021.105310>.
- [4] E.P.A. Van Langerak, H.V.M. Hamelers, G. Lettinga, Influent calcium removal by crystallization reusing anaerobic effluent alkalinity, *Water Sci. Technol.* 36 (1997) 341–348, [https://doi.org/10.1016/S0273-1223\(97\)00541-6](https://doi.org/10.1016/S0273-1223(97)00541-6).
- [5] S. Wu, S. Zou, G. Liang, G. Qian, Z. He, Enhancing recovery of magnesium as struvite from land fill leachate by pretreatment of calcium with simultaneous reduction of liquid volume via forward osmosis, *Sci. Total Environ.* 610–611 (2018) 137–146, <https://doi.org/10.1016/j.scitotenv.2017.08.038>.
- [6] Y.M. Lin, T. Lotti, P.K. Sharma, M.C.M. Van Loosdrecht, Apatite accumulation enhances the mechanical property of anammox granules, *Water Res.* 47 (2013) 4556–4566, <https://doi.org/10.1016/j.watres.2013.04.061>.
- [7] H. Ma, Y. Xue, Y. Zhang, T. Kobayashi, K. Kubota, Y. Li, Simultaneous nitrogen removal and phosphorus recovery using an anammox expanded reactor operated at 25 °C, *Water Res.* (2020), 115510, <https://doi.org/10.1016/j.watres.2020.115510>.
- [8] Y. Hwan Kim, K. Cheol, W. Kwon, Removal of organics and calcium hardness in liner paper wastewater using UASB and CO₂ stripping system, *Process Biochem.* 38 (2003) 925–931.
- [9] M. Dudziak, E. Kudlek, Removal of hardness in wastewater effluent, architecture civilengineering environment, *Arch., Civil Eng., Environ.* 2 (2019) 141–147, <https://doi.org/10.21307/ACEE-2019-030>.
- [10] Y. Guo, Y. Li, Hydroxyapatite crystallization-based phosphorus recovery coupling with the nitrogen removal through partial nitritation/anammox in a single reactor, *Water Res.* 187 (2020), <https://doi.org/10.1016/j.watres.2020.116444>.
- [11] E.P.A. Van Langerak, H. Ramaekers, J. Wiechers, H.V.M. Hamelers, G. Lettinga, Impact of location of CaCO₃ precipitation on the development of intact anaerobic sludge, *Water Res.* 34 (2000) 437–446.
- [12] Y. Xue, H. Ma, Z. Kong, Y. Guo, Y. Li, Bulking and floatation of the anammox-HAP granule caused by low phosphate concentration in the anammox reactor of expanded granular sludge bed (EGSB), *Bioresour. Technol.* 310 (2020), 123421, <https://doi.org/10.1016/j.biortech.2020.123421>.
- [13] A.A. Van De Graaf, P. De Bruijn, L.A. Robertson, M.M. Jetten, J.G. Kuenen, Autotrophic growth of anaerobic ammonium-oxidizing micro-organisms in a fluidized bed reactor, *Microbiology* 142 (1996) 2187–2196.
- [14] W.R. Abma, W. Driessen, R. Haarhuis, M.C.M. Van Loosdrecht, Upgrading of sewage treatment plant by sustainable and cost-effective separate treatment of

- industrial wastewater, *Water Sci. Technol.* 61 (2010) 1715–1722, <https://doi.org/10.2166/wst.2010.977>.
- [15] L. Van Niftrik, W.J.C. Geerts, E.G. Van Donselaar, B.M. Humbel, R.I. Webb, J. A. Fuerst, A.J. Verkleij, M.S.M. Jetten, M. Strous, Linking ultrastructure and function in four genera of anaerobic Ammonium-Oxidizing Bacteria: cell plan, glycogen storage, and localization of cytochrome c proteins, *J. Bacteriol.* 190 (2008) 708–717, <https://doi.org/10.1128/JB.01449-07>.
- [16] T. Lotti, R. Kleerebezem, C. Lubello, M.C.M. Van Loosdrecht, Physiological and kinetic characterization of a suspended cell anammox culture, *Water Res* 60 (2014) 1–14, <https://doi.org/10.1016/j.watres.2014.04.017>.
- [17] T. Lotti, W.R.L. Van Der Star, R. Kleerebezem, C. Lubello, M.C.M. Van Loosdrecht, W.R.L. van der Star, R. Kleerebezem, C. Lubello, M.C.M. van Loosdrecht, The effect of nitrite inhibition on the anammox process, *Water Res* 46 (2012) 2559–2569, <https://doi.org/10.1016/j.watres.2012.02.011>.
- [18] A. Dapena-mora, J.L. Campos, A. Mosquera-corral, R. Mendez, Stability of the ANAMMOX process in a gas-lift reactor and a SBR, *J. Biotechnol.* 110 (2004) 159–170, <https://doi.org/10.1016/j.jbiotec.2004.02.005>.
- [19] APHA, APHA: Standard methods for the examination of water and wastewater, 21st ed., Washington DC, 2005.
- [20] APAT, IRSA CNR, IRSA-CNR Metodi analitici per le acque, 2003.
- [21] FAO, Standard operating procedure for soil calcium carbonate equivalent. Titrimetric method, Rome, 2020.
- [22] H. Tiessen, T. Roberts, J. Stewart, Carbonate Analysis in soils and minerals by acid digestion and two end-point titration, *Comm. Soil Sci. Plant Anal.* 14 (1983) 161–166.
- [23] L. Mazzoli, G. Munz, T. Lotti, M. Ramazzotti, A novel universal primer pair for prokaryotes with improved performances for anammox containing communities, *Sci. Rep.* (2020) 1–7, <https://doi.org/10.1038/s41598-020-72577-4>.
- [24] S. Takahashi, J. Tomita, K. Nishioka, T. Hisada, M. Nishijima, Development of a Prokaryotic Universal Primer for Simultaneous Analysis of Bacteria and Archaea Using Next-Generation Sequencing, *PLoS One* 9 (2014), <https://doi.org/10.1371/journal.pone.0105592>.
- [25] E. Niccolai, E. Russo, S. Baldi, F. Ricci, G. Nannini, M. Pedone, F.C. Stingo, A. Taddei, M.N. Ringressi, P. Bechi, A. Mengoni, R. Fani, G. Bacci, C. Fagorzi, C. Chiellini, D. Prisco, M. Ramazzotti, A. Amedei, Significant and conflicting correlation of IL-9 with Prevotella and Bacteroides in human 2 colorectal cancer, Preprint Version (2020), <https://doi.org/10.1101/2020.04.28.066001>.
- [26] L. Tjihuis, M.C.M. Van Loosdrecht, Solids retention time in spherical biofilms in a biofilm airlift suspension reactor, *Biotechnol. Bioeng.* 44 (1994) 867–879.
- [27] X. Lin, Y. Wang, Microstructure of anammox granules and mechanisms endowing their intensity revealed by microscopic inspection and rheometry, *Water Res* (2017), <https://doi.org/10.1016/j.watres.2017.04.053>.
- [28] J.P. Gustafsson, Visual MINTEQ 3. 1 user guide, 2014: 1–73.
- [29] H. Chen, C. Ma, G. Yang, H. Wang, Z. Yu, R. Jin, Floatation of flocculent and granular sludge in a high-loaded anammox reactor, *Bioresour. Technol.* 169 (2014) 409–415, <https://doi.org/10.1016/j.biortech.2014.06.063>.
- [30] W. Li, P. Zheng, J. Ji, M. Zhang, J. Guo, J. Zhang, G. Abbas, Bioresource Technology Floatation of granular sludge and its mechanism: A key approach for high-rate denitrifying reactor, *Bioresour. Technol.* 152 (2014) 414–419, <https://doi.org/10.1016/j.biortech.2013.11.056>.
- [31] C. Chen, Y. Jiang, X. Zou, M. Guo, H. Liu, M. Cui, T.C. Zhang, Journal of Water Process Engineering Insight into the influence of particle sizes on characteristics and microbial community in the anammox granular sludge, *J. Water Process Eng.* 39 (2021), 101883, <https://doi.org/10.1016/j.jwpe.2020.101883>.
- [32] L. Chen, H. Chen, D. Lu, X. Xu, L. Zhu, Response of methanogens in calcified anaerobic granular sludge: Effect of different calcium levels, *J. Hazard. Mater.* (2020), 122131, <https://doi.org/10.1016/j.jhazmat.2020.122131>.
- [33] B. Arrojo, J.L. Campos, Effects of mechanical stress on Anammox granules in a sequencing batch reactor (SBR), *J. Biotechnol.* 123 (2006) 453–463, <https://doi.org/10.1016/j.jbiotec.2005.12.023>.
- [34] D. Kang, L. Guo, Q. Hu, D. Xu, T. Yu, Y. Li, Z. Zeng, W. Li, Surface convexity of anammox granular sludge: Digital characterization, state indication and formation mechanism, *Environ. Int.* 131 (2019), 105017, <https://doi.org/10.1016/j.envint.2019.105017>.
- [35] J.J. Heijnen, M.C.M. Van Loosdrecht, L. Tjihuis, A Black Box Mathematical Model to Calculate Auto- and Heterotrophic Biomass Yields Based on Gibbs Energy Dissipation, *Biotechnol. Bioeng.* Vol. 40 (1992) 1139–1154.
- [36] Q. Hu, D. Kang, R. Wang, A. Ding, G. Abbas, M. Zhang, Characterization of oligotrophic AnAOB culture: morphological, physiological, and ecological features, *Environ. Biotechnol.* (2018) 995–1003, <https://doi.org/10.1007/s00253-017-8587-8>.
- [37] W.F. Langelier, The analytical control of anti-corrosion water treatment, *Am. Water Work Assoc.* 28 (1936) 1500–1521.
- [38] C. Trigo, J.L. Campos, J.M. Garrido, R. Mendez, Start-up of the Anammox process in a membrane bioreactor, *J. Biotechnol.* 126 (2006) 475–487, <https://doi.org/10.1016/j.jbiotec.2006.05.008>.
- [39] W. Zhang, D. Wang, Y. Jin, Effects of inorganic carbon on the nitrous oxide emissions and microbial diversity of an anaerobic ammonia oxidation reactor, *Bioresour. Technol.* (2017), <https://doi.org/10.1016/j.biortech.2017.11.027>.
- [40] S. Johansson, M. Ruscalleda, J. Colprim, Phosphorus recovery through biologically induced precipitation by partial nitrification-anammox granular biomass, *Chem. Eng. J.* 327 (2017) 881–888, <https://doi.org/10.1016/j.cej.2017.06.129>.
- [41] B. Pagliaccia, E. Carretti, M. Severi, D. Berti, C. Lubello, T. Lotti, Heavy metal biosorption by Extracellular Polymeric Substances (EPS) recovered from anammox granular sludge, *J. Hazard. Mater.* (2021), 126661, <https://doi.org/10.1016/j.jhazmat.2021.126661>.
- [42] Y.S. Lee, W. Park, Enhanced calcium carbonate - biofilm complex formation by alkali - generating Lysinibacillus boronitolerans YS11 and alkaliphilic Bacillus sp. AK13, *AMB Express* (2019), <https://doi.org/10.1186/s13568-019-0773-x>.
- [43] M. Oshiki, H. Satoh, S. Okabe, Minireview Ecology and physiology of anaerobic ammonium oxidizing bacteria, *Environ. Microbiol.* (2016), <https://doi.org/10.1111/1462-2920.13134>.